MMP-8 Is Critical for Dexamethasone Therapy in Alkali-Burned Corneas Under Dry Eye Conditions

FANG BIAN[1], **CHANGJUN WANG**[1], **JOHANNA TUKLER-HENRIKSSON**[1], **STEPHEN C. PFLUGFELDER**[1], **CATERINA CAMODECA**[3], **ELISA NUTI**[2], **ARMANDO ROSSELLO**[2], **DE-QUAN LI**[1], and **CINTIA S. DE PAIVA**[1,*]

[1]Department of Ophthalmology, Baylor College of Medicine, Houston, Texas

[2]Department of Pharmacy, Pisa University, Pisa, Italy

[3]Division of Immunology, Transplants and Infectious Diseases, San Raffaele Scientific Institute, Milan, Italy

Abstract

Our previous studies have shown that Dexamethasone (Dex) reduced the expression of matrix-metalloproteinases (MMPs -1,-3,-9,-13), IL-1β and IL-6, while it significantly increased MMP-8 mRNA transcripts in a concomitant dry eye and corneal alkali burn murine model (CM). To investigate if MMP-8 induction is responsible for some of the protective effects of Dex in CM, MMP-8 knock out mice (MMP-8KO) were subjected to the CM for 2 or 5 days and topically treated either with 2 μl of 0.1% Dexamethasone (Dex), or saline QID. A separate group of C57BL/6 mice were topically treated with Dex or BSS and received either 100 nM CAM12 (MMP-8 inhibitor) or vehicle IP, QD. Here we demonstrate that topical Dex treated MMP-8KO mice subjected to CM showed reduced corneal clarity, increased expression of inflammatory mediators (IL-6, CXCL1, and MMP-1 mRNA) and increased neutrophil infiltration at 2D and 5D compared to Dex treated WT mice. C57BL/6 mice topically treated with Dex and CAM12 IP recapitulated findings seen with MMP-8KO mice. These results suggest that some of the anti-inflammatory effects of Dex are mediated through increased MMP-8 expression.

Chemical injuries to the cornea are a serious clinical problem, which may threaten vision or lead to loss of the eye. These injuries account for 3–4% of occupational injuries and 7–18% of ocular trauma in the United States, with young men at greatest risk (Schrage et al., 2011). The clinical outcomes of ocular burns depends not only on the severity of the injury, but also on how promptly proper treatment is initiated. Although a complete understanding of the pathogenesis of wound healing process has not been fully elucidated, there is increasing evidence that inflammatory cells, stromal cells, and corneal epithelial cells are involved in post-alkali injury tissue damage and reparative response, leading to increased expression of

inflammatory cytokines and MMPs. Despite various treatment options available, visual outcomes remain poor. Thus, better understanding of the inflammatory wound healing process is essential to improve therapeutic outcomes.

Matrix-metalloproteinases (MMPs) are key effectors and regulators of inflammation, cell migration, wound healing, and tissue remodeling pathogenic processes (Weaver et al., 2005; Gutierrez-Fernandez et al., 2007; Goldring et al., 2011). Increased production and reactivity of MMPs have been observed in corneal wound healing processes (Lyu and Joo, 2006). Topical corticosteroid has been found to effectively control acute inflammation and balance of MMPs after ocular chemical injuries (Tewari-Singh et al., 2012). However, the regulation of this inflammatory cytokine and MMPs by corticosteroids has not been thoroughly investigated. Our previous studies have shown that Dexamethasone (Dex) can reduce expression of certain inflammatory cytokines for example (IL-1β, IL-6) and MMPs (MMPs -1, -3, -9, -13) and limiting neutrophil infiltration in a combined model of alkali burn and dry eye (Bian et al., 2016). Interestingly, an impressive increase in MMP-8 was noted in this model in the group treated with topical Dex.

MMP-8, a collagen cleaving enzyme, produced by neutrophils and epithelial cells under inflammatory conditions, has been implicated in numerous tissue remodeling processes (Balbin et al., 1998; Henle et al., 2005; Chen et al., 2007). Conflicting results have been reported concerning the effect of MMP-8 on wound healing. Following cutaneous wound injury, MMP-8KO mice exhibit a significant delay in wound closure and re-epithelialization, with a delay of neutrophil infiltration during the first days and sustained inflammatory response at later time points (Gutierrez-Fernandez et al., 2007; Astrom et al., 2014) observed delayed healing of skin wounds of male MMP-8KO compared to WT, however tongue wounds of MMP-8 deficient mice closed faster at an early stage, had no change in myeloperoxidase positive myeloid cell count and had a significantly increased level of transforming growth factor-β1.

We hypothesized that Dex induced MMP-8 expression protects the cornea from alkali-induced injury. To investigate the role of MMP-8 in the Dex treatment effect, we examined the expression of inflammatory cytokines and MMPs, neutrophil infiltration, corneal opacity as well as rate of epithelial wound healing in MMP-8KO in our combined model of alkali burn and dry eye. The effects of a systemic MMP-8 inhibitor on corneal wound healing were also evaluated. Genetic deletion or inhibition of MMP-8 were found to worsen corneal healing in a combined model of alkali burn/dry eye. Greater understanding of the pharmacological activity of Dex in this model provides new insight into corneal wound healing and may improve treatment outcomes for patients with ocular burn.

Materials and Methods

Combined model of alkali burn and dry eye

This research protocol was approved by the Baylor College of Medicine Center for Comparative Medicine, and it conformed to the standards in the ARVO Statement for the use of animals in Ophthalmic and Vision Research. Female C57BL/6 were purchased from Jackson Laboratories (Bar Harbor, ME) and used at 6–8 weeks of age. MMP-8KO were

purchased from Jackson Laboratories for establishing of a breeding colony at Baylor College of Medicine Comparative Medicine Facility.

Unilateral alkali burn (AB) was created on a right eye of female C57BL/6 or MMP-8KO mice after systemic anesthesia with isoflurane using a vaporizer (SomnoSuite, Kent Scientific, Torrington), by placing one 2.0 mm diameter filter paper disc presoaked with 1 N NaOH on the central cornea for 10 sec, followed by extensive rinsing with balanced salt solution (Alcon, Fort Worth, TX), as previously described (Bian et al., 2015). Precautions were taken to avoid damage of peripheral cornea, conjunctiva, and lids. After anesthetic recovery, mice were subjected to desiccating stress (DS) for 2 or 5 days (referred to as the combined model of alkali burn and DS = CM).

DS was induced in female C57BL/6 or MMP-8KO mice aged 6–8 weeks by sterile subcutaneous injection of 0.5 mg/1 ml scopolamine hydrobromide (Sigma–Aldrich, St. Louis, MO) QID into alternating flanks and exposure to a drafty low humidity (<30% relative humidity) environment for 2 or 5 days as previously described (De Paiva et al., 2009).

Dosing regiments

Naïve or mice subjected to the combined model of alkali burn and dry eye were topically or systemically treated as described below. Tissues were collected after 2 or 5 days post-initial injury.

Topical anti-inflammatory therapy—C57BL/6 or MMP-8 KO mice subjected to the CM of alkali burn and dry eye were topically treated either with 2 μl sodium phosphate Dexamethasone (Dex, 0.1%, Spectrum Laboratory, Gardena, CA), or vehicle (balanced salt solution, BSS, Alcon, Fort Worth, TX) QID.

Systemic MMP-8 inhibitor in naïve control mice—To investigate if MMP-8 inhibitor had an inflammatory effect, naïve C57BL/6 mice received either 100 nM CAM12 (a MMP-8 inhibitor) or vehicle (Phosphate buffered saline, PBS) intraperitoneal injection (IP), Q.D for 2 and 5 days.

Topical anti-inflammatory therapy combined with systemic MMP-8 inhibitor—A separate group of C57BL/6 mice were subjected to CM, received topical treatment (Dex or BSS) and received either 100 nM CAM12 (a MMP-8 inhibitor) or vehicle (Phosphate buffered saline, PBS) intraperitoneal injection (IP), Q.D for 2 and 5 days after initial injury and were compared to naïve control corneas.

One hundred and seventy C57BL/6 mice and 110 MMP-8KO mice were used in this study. Twenty two MMP8KO or C57BL/6 animals without corneal perforations were used per group (BSS or Dex) and per time point (2D, 5D): six for histology, twelve for real-time PCR, and four for myeloperoxidase assay. Corneal opacity and wound closure rate were evaluated in twelve live mice that were used for either histology or PCR. Twenty two naïve animals (no burn, no dry eye) were used as untreated controls.

For the MMP-8 inhibitor experiment, twelve C57BL/6 animals without corneal perforations were used per group (BSS or Dex) and per time point (2D, 5D) for real-time PCR. These mice also received systemic IP injection of MMP-8 inhibitor or its vehicle (PBS) in additional to its topical treatment. Corneal opacity and wound closure rate were evaluated in twelve live mice that were used for PCR.

Clinical findings: Opacity score

Biomicroscopic examination was used to grade corneal edema and opacity by two masked observers in images taken by a color digital camera DS-Fi1 (Melville, NY) by the way described by Yoeruek et al. (2008). Corneal opacity was scored using a scale of 0–4 where grade 0 = completely clear; grade 1 = slightly hazy, iris, and pupils easily visible; grade 2 = slightly opaque, iris, and pupils still detectable; grade 3 = opaque, pupils hardly detectable, and grade 4 = completely opaque with no view of the pupils.

Measurement of corneal epithelial defect

Corneal epithelial healing was assessed daily in the experimental groups (four mice per group per experiment; three sets of experiments). Briefly, 1 μl of 0.1% liquid sodium fluorescein was instilled onto the ocular surface. Corneas were rinsed with phosphate-buffered saline and photographed with a stereoscopic zoom microscope (SMZ 1500; Nikon, Melville, NY) under fluorescence excitation at 470 nm (digital camera DS-Qi1Mc, Nikon). Corneal epithelial defect area was graded in digital images by two masked observers in a categorical manner (present/absent) to generate a survival curve (Bian et al., 2015). Biological replicate scores were transferred to excel database and results analyzed.

Histology and immunostaining

For immunohistochemistry, eyes and adnexae from each group/time point (n = 6/group) were excised, embedded in optimal cutting temperature compound (VWR, Suwanee, GA), and flash frozen in liquid nitrogen. Sagittal 8 μm tissue sections were cut with a cryostat (HM 500; Micron, Waldorf, Germany) and placed on glass slides that were stored at −80°C. Immunohistochemistry was performed to detect neutrophils using rat anti-Gr-1 antibody (Ly6G; 1:250, clone 1A8, BD Pharmingen, San Diego, CA). Cryosections were stained with the primary antibody and appropriate biotinylated secondary antibody (1:100 biotin goat α-rat, BD Pharmingen) using a Vectastain Elite ABC kit and Nova Red reagents (Vector, Burlingame, CA). Six sections from each animal/group/time point were examined and photographed with microscope equipped with a digital camera (Eclipse E400 with a DS-Qi1Mc; Nikon). The numbers of Gr-1 positive (+) cells were counted in cornea sections from each animal at 20× magnification and results averaged and expressed as the number of positive cells per cornea.

Immunofluorescent staining was performed in frozen tissue sections with rabbit polyclonal antibody anti-MMP-1 (1:100, ab-137332; Abcam, Cambridge, MA) and anti-IL-1β (1:100, #12426 Cell Signaling). Secondary goat-anti rabbit Alexa-Fluor 488 conjugated IgG antibodies were used, as previously described (Corrales et al., 2006). The images were captured and photographed by a Nikon fluorescence microscope (Eclipse E400 equipped with a DS-F1 digital camera; Nikon).

RNA isolation and quantitative PCR

Four whole corneas/group/time point/per experiment were excised, minced, and total RNA was extracted using a Qiagen MicroPlus RNeasy isolation® Kit (Qiagen, Valencia, CA) according to the manufacturer's instructions, quantified by a NanoDrop® ND-2000 Spectrophotometer (Thermo Scientific, Wilmington, DE) and stored at −80°C. First-strand cDNA was synthesized with random hexamers by M-MuLV reverse transcription (Ready-To-Go You-Prime First-Strand Beads; GE Healthcare, Inc., Arlington Heights, NJ), as previously described (Luo et al., 2004).

Real-time polymerase chain reaction (PCR) was performed with specific Taqman MGB probes (Applied Biosystems, Inc., Foster City, CA) and PCR master mix (Taqman Gene Expression Master Mix), in a commercial thermocycling system (StepOnePlus™ Real-Time PCR System, Applied Biosystems), according to the manufacturer's recommendations. Quantitative real time PCR was performed using gene expression assay primers and MGB probes specific for murine targets described in Table 1. The beta-2-microglobulin (B2M) gene was used as an endogenous reference for each reaction to correct for differences in the amount of total RNA added. The results of quantitative PCR were analyzed by the comparative C_T method where target $\mathrm{change} = 2^{-\Delta\Delta_T^C}$. The results were normalized by the C_T value of B2M and the relative mRNA level in the naïve control group was used as the calibrator.

Myeloperoxidase assay

Myeloperoxidase (MPO) activity was measured using a myeloperoxidase colorimetric activity assay kit as described by the manufacturer (Sigma–Aldrich). Briefly, whole cornea lysates (n = 4/group/time point/experiment) were homogenized in MPO assay buffer and the homogenate was centrifuged at $14,000g$ for 20 min at 4°C. Total protein concentration was measured by the BCA protein assay as previously described (De Paiva et al., 2009). Fifty microgram per sample was mixed with MPO assay buffer and MPO substrate, incubated at room temperature for 2 h, and then mixed with tetramethylbenzidine probe. Fluorescence was measured at 412 nm using a Tecan Infinite M200 plate reader equipped with Magellan V6.55 software. Biologic replicate samples were averaged. Results are presented as mean ± SEM (milliunits).

MMP-8 inhibitor synthesis

Melting points were determined on a Kofler hotstage apparatus and are uncorrected. ^{1}H and ^{13}C NMR spectra were determined with a Bruker Avance III HD 400 MHz spectrometer. Chemical shifts (δ) are reported in parts per million downfield from tetramethylsilane and referenced from solvent references. Coupling constants J are reported in hertz; ^{13}C NMR spectra were fully decoupled. The following abbreviations are used: singlet (s), doublet (d), triplet (t), doubledoublet (dd), broad (br), and multiplet (m). Chromatographic separations were performed on silica gel columns by flash column chromatography (Kieselgel 40, 0.040–0.063 mm; Merck & Co. Rome, Italy) or using ISOLUTE flash Si II cartridges (Biotage). Reactions were followed by thin-layer chromatography (TLC) on Merck aluminum silica gel (60 F254) sheets that were visualized

under a UV lamp, and hydroxamic acids were visualized with $FeCl_3$ aqueous solution. Evaporation was performed in vacuo (rotating evaporator). Sodium sulfate was always used as the drying agent. Commercially available chemicals were purchased from Sigma–Aldrich.

Benzyl 2-((4-bromophenyl) sulfonyl) benzoate (2)—A solution of Oxone (12.32 g, 20 mmol) in water (48 ml) was added slowly to a solution of benzyl 2-(4-bromophenylthio) benzoate **1** (1 g, 2.50 mmol) in THF/MeOH (3:1, 48 ml). The reaction was stirred at room temperature for 5 days, and the organic solvents were evaporated under reduced pressure. The obtained suspension was diluted with H_2O, and the product was extracted with EtOAc. The combined organic extracts were dried over anhydrous Na_2SO_4, filtered and evaporated under reduced pressure. The crude oil was purified by trituration with Et_2O/*n-hexane* to yield **2** as a white solid (980 mg, 91% yield). ^{1}H NMR ($CDCl_3$) δ: 5.39 (s, 2H), 7.36–7.44 (m, 5H), 7.51–7.56 (m, 2H), 7.58–7.65 (m, 3H), 7.77–7.81 (m, 2H), 8.11–8.15 (m, 1H).

Benzyl 2-((4′-morpholino-[1,1′-biphenyl]-4-yl) sulfonyl) benzoate (3)—A solution of $Pd(OAc)_2$ (6.5 mg, 0.029 mmol) and triphenylphosphine (37 mg, 0.140 mmol) in ethanol (2 ml) and toluene (2 ml) was stirred at room temperature under inert atmosphere for 15 min. Benzyl 2-((4-bromophenyl) sulfonyl) benzoate (420 mg, 0.97 mmol), an aqueous solution of Na_2CO_3 (3 ml, 2 M) and (4-morpholinophenyl) boronic acid (242 mg, 1.17 mmol) were then added and the reaction was stirred under reflux (85°C) for 3 h. After cooling to rt, the obtained suspension was diluted with water and extracted with EtOAc. The combined organic extracts were dried over anhydrous Na_2SO_4, filtered and evaporated under reduced pressure. The crude product was purified by flash chromatography (n-hexane/ EtOAc 3:1) using a ISOLUTE Flash Si II cartridge (10 g) to give the pure compound 3 (267 mg, 65% yield) as a pale yellow solid. ^{1}H NMR ($CDCl_3$) δ: 3.21–3.26 (m, 4H), 3.87–3.92 (m, 4H), 5.42 (s, 2H), 6.97–7.02 (m, 2H), 7.33–7.63 (m, 12H), 7.93–7.98 (m, 2H), 8.11–8.16 (m, 1H).

2-((4′-Morpholino-[1,1′-biphenyl]-4-yl) sulfonyl) benzoic acid (4)—To a suspension of the ester 3 (261 mg, 0.51 mmol) in H_2O (1.6 ml), THF (1 ml), and KOH (86 mg, 1.53 mmol) were added, the reaction was stirred under reflux (100°C) overnight. After cooling to room temperature the mixture was acidified with HCl 1N (pH 4) and extracted with EtOAc. The combined organic layers were dried over anhydrous Na_2SO_4, filtered and evaporated under reduced pressure. The solid thus obtained was purified by trituration with CH_2Cl_2 to afford the pure compound **4** as a pale yellow solid (170 mg, 79% yield); mp 205–207°C. ^{1}H NMR (DMSO-d_6) δ: 3.16–3.21 (m, 4 H), 3.72–3.76 (m, 4 H), 7.00–7.09 (m, 2 H), 7.62–7.65 (m, 3H), 7.74–7.78 (m, 2H), 7.84–7.86 (m, 2H), 7.97–8.00 (m, 2H), 8.15–8.18 (m, 1H), 13.6 (brs, 1H). C NMR (DMSO-d_6) δ: 48.19, 66.45, 115.49, 126.59, 128.26, 128.55, 128.91, 129.02, 130.18, 131.13, 134.35, 138.15, 138.85, 145.31, 151.78, 168.89.

N-Hydroxy-2-((4′-morpholino-[1,1′-biphenyl]-4-yl) sulfonyl) benzamide (CAM12)—1-[3-(Dimethylamino) propyl]-3-ethyl carbodiimide hydrochloride (EDC) was added portionwise (88 mg, 0.46 mmol) to a stirred solution of benzoic acid **4** (130 mg, 0.31 mmol) and *O*-(*tert*-butyldimethylsilyl) hydroxylamine (68 mg, 0.46 mmol), in anhydrous THF (15 ml). After stirring at room temperature overnight, the organic solvent was

evaporated under reduced pressure, the residue was diluted with water and extracted with CH_2Cl_2. The combined organic extracts were dried over Na_2SO_4, filtered and evaporated under reduced pressure. The crude product was purified by flash chromatography (*n*-hexane/ EtOAc 1:1) using a ISOLUTE Flash Si II cartridge (5 g) to afford the *O*-silylate intermediate (60 mg, 34% yield).

TFA (57 equiv) was added dropwise to a stirred and ice-chilled solution of *O*-silylate intermediate (1 equiv) in dry CH_2Cl_2 (8 ml/mmol). The solution was stirred under this conditions for 5 h, and then the solvent was removed in vacuo. The crude product was purified by trituration with Et_2O to give the hydroxamic acid CAM12 as a white solid (67 mg, 95% yield); mp 156–158 °C. ^1H NMR (DMSO-d_6) δ: 3.18–3.21(m,4 H),3.74–3.76(m, 4H),7.03–7.06(m,2H),7.42–7.44(m, 1H), 7.63–7.66 (m, 2H), 7.69–7.72 (m, 2H), 7.82–7.84 (m, 2H), 8.04–8.06 (m, 2H), 8.12–8.15 (m, 1H), 9.22 (brs, 1H), 10.94 (s, 1H). ^{13}C NMR (DMSO-d_6) δ: 48.21, 66.46, 115.50, 126.50, 128.25, 128.66, 129.20, 130.19, 130.38, 130.98, 134.09, 135.45, 139.14, 139.27, 145.26, 151.76, 164.62.

MMP inhibition assays

The fluorogenic peptides FS6 (Mca-Lys-Pro-Leu-Gly-Leu-Dap(Dnp)-Ala-Arg-NH2) and M-9545 (Mca-Arg-Pro-Lys-Pro-Val-Glu-Nva-Trp-Arg-Lys(Dnp)-NH2) were purchased respectively from Bachem (Bubendorf, Switzerland) and Sigma–Aldrich (Milano, Italy). Recombinant human pro-MMP-1, pro-MMP-2, pro-MMP-3, and pro-MMP-9 were purchased from Calbiochem (Merck Millipore). Pro-MMP-8 and MMP-14 cd were a kind gift from Professor Gillian Murphy, University of Cambridge, Cambridge, UK. APMA (p-aminophenylmercuric acetate), DMSO (dimethyl sulfoxide), and Tris base (tris(hydroxymethyl)-aminomethane) were purchased from Sigma–Aldrich. Ninety-six well microtitre plates were from Corning (Sigma–Aldrich).

All enzyme assays were conducted in Fluorimetric Assay Buffer (FAB: 50 mM Tris Base, 10 mM CaCl2, 150 mM NaCl, 1% DMSO, 0.05% Briji-35, pH 7.5) at 37°C, using a SPECTRAmax Gemini XPS microplate spectrofluorometer (Molecular Devices, Sunnyvale, CA). MMP-1, MMP-2, MMP-8, and MMP-9 pro-enzymes were activated immediately prior to use with APMA (final concentration: 2 mM for 2 h at 37°C for MMP-1, 2 mM for 1 h at 37°C for MMP-2 and MMP-8, 1 mM for 1 h at 37°C for MMP-9). Pro-MMP-3 was activated with trypsin (4.4 μg/ml) for 30 min at 37°C followed by addition of soybean trypsin inhibitor (61.5 μg/ml). MMP-14 cd was catalytically active.

Assays were performed in a total volume of 200 μl per well in 96-well microtitre plates. Stock solutions (10 mM) of the inhibitors in DMSO were further diluted in FAB for 4 h at 25°C in the presence of the activated enzyme (final concentration: 2 nM for MMP-1, 0.56 nM for MMP-2, 5 nM for MMP-3, 1.3 nM for MMP-9, 1.5 nM for MMP-8, 1 nM for MMP-14). The hydrolysis of FS6 (final concentration: 2 μM) was monitored every 5 s for 15 min at 37°C at excitation and emission wavelengths of 325 and 400 nm, respectively. For MMP-3, the substrate used was M-9545 at a final concentration of 2 μM. In this case, the excitation and emission wavelengths were 328 and 393 nm, respectively. Enzymatic rates were corrected for spontaneous hydrolysis of the substrate. IC50 values were determined using the formula vi/v0 = 1/(1 + [I]/IC50), where vi is the initial velocity of substrate

cleavage in the presence of the inhibitor at concentration [I] and v0 is the initial velocity in the absence of the inhibitor. Results were analyzed using SoftMax Pro software and Prism Software version 5.0 (GraphPad Software, Inc., La Jolla, CA).

Statistical analysis

Results are presented as the mean ± SEM. Two-way analysis of variance (ANOVA) with Bonferroni post hoc testing was used for statistical comparisons of gene expression. P 0.05 was considered statistical significant. These tests were performed using GraphPad Prism 6.0 software (GraphPad Incorporation).

Results

Dexamethasone increased MMP-8 production in the combine model of alkali burn of dry eye associated with desiccating stress

MMPs are key regulators of wound healing response to injury. MMP-8 is mainly produced by neutrophils, but has been found in the other cells such as inflamed lung epithelium (Prikk et al., 2001). We previously found significantly increased MMP-8 expression and decreased neutrophil infiltration in Dex treated corneas of eyes subjected to a combined model of corneal alkali burn and dry eye (Bian et al., 2016). As shown in Table 2, there was a remarkable increase in MMP-8 transcripts at 2 days (up to a 2000-fold) and 5 days (up to a 300-fold) in Dex-treated corneas compared to vehicle (BSS) treated corneas. These data prompted us to investigate if stimulated MMP-8 expression may be responsible for some of the anti-inflammatory actions of Dex in this model.

Protective properties of dexamethasone in alkali burn associated with dry eye are lost in MMP-8KO mice

MMP-8 has been a particular focus of wound healing research because of its positive effect in the wound healing process (Gutierrez-Fernandez et al., 2007). Our previous studies showed that Dex treated corneas had lower opacity scores in eyes subjected to the CM (Bian et al., 2016). In our current study, we subjected MMP-8KO and WT mice to the CM model, and topically treated with either Dex or BSS and evaluated clinical parameters of wound healing and corneal opacity. Representative images of corneal opacity and wound closure are shown on Figure 1A and B. After grading corneal clarity and epithelial healing on a daily basis, we observed that Dex-treated MMP-8KO corneas had significantly higher corneal opacity scores than Dex treated WT corneas 5 days post injury (Fig. 1C). These findings are in accordance with our previous findings that Dex treated WT corneas had significantly lower opacity scores than BSS treated corneas 2D post injury (Bian et al., 2016). At 5D post injury, Dex treated MMP-8 KO corneas had similar opacity scores as BSS treated WT, indicating that MMP-8 participates in the protective role of Dex in preserving corneal clarity.

The corneal wound closure rate in WT was similar in both Dex and BSS-treated mice the first 2 days post injury (Fig. 1D). Dex treated MMP-8KO mice exhibited delayed wound healing, with only 40% wound healing by day 5 in comparison to Dex treated WT animals

which healed by 75% at day 5. This data suggests that loss of MMP-8 may be responsible for delayed corneal wound healing in the Dex-treated group.

Dexamethasone has less anti-inflammatory effects in MMP-8KO mice

Dexamethasone, a prototype glucocorticosteroid, has been known to exert its anti-inflammatory effects by regulating inflammatory factors, including MMPs (Saadat et al., 2005; Previti et al., 2006; Saraiya and Goldstein, 2011). Our previous studies have shown that early treatment with Dex is very efficacious in controlling MMP production and migration of neutrophils (Bian et al., 2016). To test the hypothesis that Dex is less-effective in controlling inflammation in MMP-8 deficient mice, we examined the expression of MMP -1, -3, -9, -13, and IL-6 in the corneas subjected to the CM model and topically treated with either Dex or its vehicle in both WT and MMP-8KO mice by qPCR. As shown in Figure 2A, treatment with BSS in both WT and MMP-8 KO mice had higher expression of IL-6, MMPs -1,-3,-9,-13 mRNA at 2D and 5D compared to naïve corneas. Interestingly, MMP-8KO mice treated with BSS had higher IL-6 transcripts and lower MMP-9, -13 transcripts compared with WT corneas treated with BSS. Dex treatment in WT significantly decreased IL-6, MMPs -3, -9, -13 transcripts at 2D post injury and significantly decreased IL-6 and MMP-3 at 5D. Although Dex-treated MMP-8KO have decreased IL-6, MMP-3, and MMP-9 at 2D post injury and decreased MMP-9 and MMP-13 at 5D post injury compared to BSS-treated MMP-8KO mice. However, IL-6 and MMP-1 transcripts were significantly lower in Dex treated WT compared with MMP8-KO with the same treatment.

Immunoreactivity of corneas to MMP-1 was evaluated by immunostaining (Fig. 2B). Minimal levels of MMP-1 were present in the control corneas. Increased reactivity against MMP-1 was noted in apical corneal epithelial cells in BSS treated corneas in both MMP-8KO and WT at 2D and 5D. Topical Dex treatment decreased MMP-1 immunoreactivity by corneal epithelium in WT, but not in MMP-8KO. Consistent with the PCR results, Dex lost its ability to suppress MMPs and IL-6 by the corneal epithelium.

The accumulation of neutrophils was reduced in wounded corneas of MMP-8KO mice subjected to the CM model

Neutrophils, human body's first line defense, are well recognized as one of the major players during acute inflammation (Kolaczkowska and Kubes, 2013). Dex has been reported to inhibit neutrophil recruitment to a site of inflammation such as the newborn lung with bronchopulmonary dysplasia (Zentay et al., 1999). Chemokines recruit a variety of inflammatory cells, including neutrophils into the wound site (Kolaczkowska and Kubes, 2013). It has been showed that IL-1β deficient mice have defective systemic and local neutrophil mobilization (Biondo et al., 2014b). C-X-C motif ligand 1 (CXCL1) has been shown to promote neutrophil migration (Biondo et al., 2014a). As we previously reported, rapid release of IL-1β and CXCL1, and the migration of neutrophils into the wound site was seen in the CM. Dex treatment following CM significantly decreased IL-1β and CXCL1 expression compared to BSS vehicle 2D post injury in WT (Bian et al., 2016).

In order to investigate whether Dex would decreased chemokine release from neutrophils, we assessed IL-1β and CXCL1 expression by PCR and immunohistochemistry in WT and

MMP-8KO mice subjected to the CM and topical treatment with Dex. In contrast to WT, Dex lost its ability to decrease IL-1β and CXCL1 expression in MMP-8 KO (Fig. 3A), and these findings for IL-1β expression were confirmed by immunofluorescent staining (Fig. 3B).

To evaluate neutrophil infiltration in the wound site, we performed immunohistochemistry of wounded tissue at different time points using Gr-1 antibody (Fig. 3C and D). Consistent with our previous results, a significant influx of Gr-1^{+} cells into the wound site was observed in BSS treated corneas in WT mice at 2D and 5D. Dex inhibited the influx of Gr-1^{+} cells into the wound site in WT mice, but not in MMP-8KO mice.

Myeloperoxidase (MPO), an enzyme mostly abundantly expressed in neutrophil granulocytes, has been used as a measure of neutrophil infiltration (Ji et al., 2008). As shown in Figure 3E, topical Dex significantly decreased MPO activity from 9.4 to 5.1 mU, reaching levels found in naïve WT mice. Although Dex significantly decreased MPO activity compared to BSS in MMP-8KO mice, it was still significantly higher than WT Dex treated corneas, indicating that MMP-8 is beneficial for Dex to suppress neutrophil infiltration. These results were consistent with Gr-1 immunohistochemistry.

Taken together, our results demonstrated that Dex can inhibit neutrophil infiltration, while decreasing expression of IL-1β and CXCL1 and increasing MMP-8 in wounded corneas.

MMP-8 inhibitor CAM12 recapitulates results seen with MMP-8KO mice

To further evaluate the participation of MMP-8 in the anti-inflammatory effects of Dex in controlling the inflammation on corneal wound healing, we used an MMP-8 inhibitor in the CM model. On the basis of previous results (Nuti et al., 2009), we have designed and synthesized CAM12, a new small molecule that selectively inhibits MMP-8 over MMP-1, MMP-3, MMP-14, and MMP-9 (Table 3). This sulfone-based benzoic hydroxamate is a zinc-chelating, competitive MMP-8 inhibitor, which inhibited MMP-8 with an IC_{50} value of 57 nM, while it inhibited MMP-1, MMP-14, and MMP-9 poorly with IC_{50} values of 16700, 1140, and 2300 nM, respectively. The hydroxamate derivative CAM12 was synthesized as described in Figure 4. Compound **1**, prepared following a previously described procedure, (Nuti et al., 2009) was oxidized to the corresponding sulfone **2** using Oxone in MeOH/THF/H_2O. A Pd-catalyzed cross-coupling reaction (under classical Suzuki conditions) of the arylbromide **2** with 4-morpholinophenylboronic acid afforded the biphenyl derivative **3**, which was converted into the corresponding carboxylic acid **4** by basic hydrolysis. Finally, the corresponding hydroxamate (**CAM12**) was obtained through condensation of the carboxylate **4** with *O*-(*tert*-butyldimethylsilyl) hydroxylamine, followed by acid hydrolysis with TFA.

To investigate whether CAM12 alone could trigger an inflammatory response, WT naïve mice received CAM12 or PBS intraperitoneal injections QD for 5D and whole corneas were harvested for PCR. Normal mice that received CAM12 IP for 5 days had no change in expression of inflammatory cytokines and MMPs in the cornea, indicating that CAM12 was safe to use in vivo (data not shown).

We next subjected WT mice to the CM model, topically treated with either Dex or BSS vehicle and systemically injected with either PBS or the MMP-8 inhibitor CAM12 for 2D or 5D. Representative images for corneal opacity and wound closure at 5D post-injury are shown on Figure 5A and B. As expected, topical Dex treatment + vehicle-injected mice had significantly lower corneal opacity compared to topical BSS treatment + vehicle-injected controls (Fig. 5C). However, topical Dex treatment + CAM12 injection had a signi ficantly higher corneal opacity score compared to Dex treatment + vehicle-injected controls. As shown in Figure 5D, topical Dex treatment + CAM12-injected mice had delayed re epithelialization compared to Dex-treated + vehicle-injected controls, suggesting that MMP-8 has a positive effect on corneal wound healing and contributes to maintenance of corneal clarity.

We next evaluated the expression of inflammatory cytokine and MMPs genes in injured corneas treated with Dex in mice receiving systemic CAM12 injection with its controls. As shown in Figure 5E, both Dex and BSS topical treatment with CAM12 IP injections had higher expression of IL-1β, IL-6, MMP-9 at 2D and 5D, compared with its controls. Furthermore, Dex topical treatment in CAM12 IP injected mice had higher levels of MMP-1, -3 at 5D and higher MMP-13 mRNA transcripts at both 2D and 5D. These data confirmed the findings in MMP-8KO mice that Dex has lower anti-inflammatory effects when MMP-8 is either blocked or genetically deleted.

Discussion

We have developed this animal model of inflammation that combines two different types of insults to the ocular surface: (1) an alkali burn, which has been to show extensively increase MMPs and inflammatory cytokines (Sosne et al., 2005; Herretes et al., 2006; Takahashi et al., 2007) and (2) desiccating stress, which has also been shown to increase MMP activity and inflammation (Pflugfelder et al., 2005; Corrales et al., 2006; de Paiva et al., 2006). The combination of these models leads to intense corneal inflammation, influx of neutrophils, upregulation of cytokines, proteases, and eventually corneal perforation (Bian et al., 2015). This model allows us to study to most severe cases of ocular injuries, simulating patients with extensive facial burns, patients in prolonged stay in environmentally controlled intensive care units (ICU) and patients with compromise of eyelids. We believe that dry eye, either by exposure of the cornea or by low humidity environments (such as ICU with controlled ambient humidity), may be an unrecognized source of inflammation in alkali burns.

In the present study, we demonstrated one of the possible mechanisms by which Dex controls inflammation in corneal wound repair by showing that MMP-8 deficient mice exhibit higher corneal opacity and higher inflammatory response following Dex treatment. Moreover, this effect was confirmed by using a specific MMP-8 inhibitor, indicating that Dex-induced MMP-8 derived from both neutrophils and corneal epithelial cells is necessary to the anti-inflammatory activity of Dex.

MMPs are important modulators of inflammation, reepithelialization and tissue remodeling and are highly expressed at wound sites. Key members of the MMP family, including

collagenases MMP-1, -8, -13, gelatinases MMP-2, -9, stromelysins MMP-3, -10, -11, and MMP-12, have been shown to be involved in the pathogenesis of corneal diseases (Fini et al., 1992; Sivak and Fini, 2002; Sakimoto and Sawa, 2012). Evidence from both human and animal studies have shown an increase in MMPs -1, -2, -3, -8, -9, and -13 expression and activity that associates with severity of corneal diseases (Ye et al., 2000; Mitchell et al., 2007; Brejchova et al., 2010). Except for participating in the cleavage of numerous substrates, MMPs also regulate inflammatory cells infiltration in wound site by regulating expression of chemokines and other cytokines (Gill and Parks, 2008). In the acute stage of corneal injury, MMP-12 deficiency results in higher expression of CXCL1, which in turn increases macrophage infiltration and decreases neutrophil infiltration following corneal injury (Chan et al., 2013). Neutrophil migration has also been reported to be impaired in a murine model of LPS keratitis in MMP-8 deficient mice through reduced chemotactic Pro-Gly-Pro production (Lin et al., 2008).

Originally regarded as neutrophil collagenase, MMP-8 was believed to be synthesized exclusively by neutrophils. However, studies have demonstrated that MMP-8 expression was also observed in diverse cell types, including epithelial cells, fibroblasts, activated macrophages, and endothelial cells (Herman et al., 2001; Tsubota et al., 2002; Zheng et al., 2002). Although elevated MMP-8 has been found in association with non-healing ulcers, delayed infiltration of neutrophils into skin wounds retards the repair process in MMP-8 deficient mice (Gutierrez-Fernandez et al., 2007). In skin wound healing of diabetic mice, MMP-8 also has been shown to have a beneficial effect. Gooyit and colleagues have shown that in the diabetic mice with wounded skin, the expression of active MMP-8 and MMP-9 were elevated from days 7 to 10 post-injury compared to the levels in the wounded tissue from wild type mice. Using a selective MMP-9 inhibitor led to acceleration of wound closure and re-epithelization while inhibition of MMP-8 delayed wound closure and decreased re-epithelialization in diabetic mice (Gooyit et al., 2014).

Dexamethasone is used to treat a variety of inflammatory conditions in various parts of the body. In eyes, FDA approved indications for Dex are inflammatory conditions of the palpebral and bulbar conjunctiva, cornea, and anterior segment of the globe as well as corneal injury (Albietz et al., 2007). Dex treatment inhibited the pro-inflammatory cytokine IL-1β-induced production of IL-6, IL-8, and GM-CSF in vitro in cultured human corneal cells (Djalilian et al., 2006). Latent and active forms of MMP-9 were inhibited by Dexamethasone in chemically burned cornea (Yi et al., 2011). Dex also was found to effectively decrease corneal opacity score following corneal transplantation and corneal trauma (Hoffart et al., 2010). Despite its anti-inflammatory potential, treatment of corneal burns with corticosteroids can delay wound healing (Chung et al., 1998). Our previous studies have demonstrated that Dex indeed preserved corneal clarity, while it slightly decreased corneal wound healing in a concomitant dry eye and corneal alkali burn murine model (Bian et al., 2016). This was accompanied by reduced expression of certain MMPs (MMPs -1, -3, -9, -12, -13) and inflammatory cytokines (IL-1β and IL-6) expression while it significantly increased MMP-8. Since Dex maintained corneal clarity despite a modest delay in corneal wound healing, we believe that its benefits for preserving corneal healing outweighs its risks because cornea clarity is critical to sight preservation after a severe corneal chemical burn. This is in agreement with the review by Hamill and colleagues who

proposed hourly administration of corticosteroids after corneal burn (Hamill et al., 2013) and demonstrated that a defined algorithm improved care and visual acuity in patients with corneal alkali burns (Al-Moujahed and Chodosh, 2015).

Among the MMPs that we evaluated in the desiccated alkali-burned corneas treated with Dex, only MMP-8 was found to be enhanced. One question which is raised by this study is whether the beneficial effects of Dex on preservation of corneal clarity and inflammation control are primarily due to MMP-8.

As expected, Dex treated corneas showed significantly improved opacity in WT mice, which is consistent with our previous results and also in agreement with Hoffart who showed Dex effectively decreased corneal opacity score at 7 days post-injury in a rat corneal chemical burn model (Hoffart et al., 2010). However, after daily monitoring corneal clarity and the corneal healing process, we observed that Dex treatment in MMP-8 deficient mice subjected to the CM model failed to preserve corneal clarity compared to WT. Failure of Dex to preserve corneal clarity in MMP-8 deficient mice indicates that MMP-8 participates in the protective role of Dex in preserving corneal clarity. In our CM model, Dex treatment of MMP-8KO corneas exhibited delayed wound healing compared with Dex treated WT mice. This finding also suggests that MMP-8 has a protective role in corneal wound healing.

To investigate whether the anti-inflammatory effects of Dex are dependent on MMP-8, we tested the expression of inflammatory cytokines (IL-1β and IL-6) and MMPs (MMPs -1, -3,-9,-13) in wounded corneas topically treated with Dex in MMP-8KO. Our results show that Dex treatment of MMP-8 deficient mice failed to decrease IL-1β transcripts and resulted in significantly higher level of IL-6, MMP-1, and CXCL1 transcripts in their corneas compared to WT mice treated with Dex. IL-6 is produced by T cells and macrophages at the site of inflammation and plays a key role in the induction of acute phase reactions.

As a first line defense, neutrophils play an important function in corneal wound healing. A cytokine circuit that involves IL-1β induced production of CXCL1/2 to recruitment of neutrophils to group B streptococcus infection sites, whereas IL-1β deficient mice had significantly decreased levels of neutrophil chemokines CXCL1 and CXCL2, and decreased neutrophil infiltration in the infection site (Biondo et al., 2014a). To study the relationship between chemokine induction and neutrophil infiltration in more detail, we measured mRNA levels of CXCL1 and IL-1β, performed IL-1β staining, counted Gr-1 positive cells and measured MPO levels. Here we show that Dex decreased IL-1β and CXCL1 expression in WT mice, but failed to reduce their expression in MMP-8KO in the CM 2D post injury. Consistent with the level of Gr-1 cell infiltration, corneas of MMP-8KO mice treated with Dex also had reduced MPO activity, although it was still much higher than the MPO level in BSS treated corneas in WT mice. These data provide evidence that the effect of Dex in limiting neutrophil infiltration in corneal wound healing are mediated in part by MMP-8.

To confirm the participation of MMP-8 in the wound healing modulation by Dex, we found that systemic administration of the MMP-8 inhibitor (CAM12) during Dex treatment in the WT mice recapitulated the phenotype observed in the MMP-8KO in two aspects. First, Dex treated WT mice receiving intraperitoneal CAM12 injections had significantly increased

corneal opacity compared to Dex treated WT vehicle control. Corneal re-epithelialization in mice receiving CAM12 and topical Dex was decreased relative to vehicle-treated Dex controls. Second, the expression of inflammatory cytokine and MMP genes in the injured corneas following topical Dex treatment in mice receiving CAM12 was significantly higher, with increase of IL-1β, IL-6, and MMP-9 at 2D and 5D, compared with Dex topically treated corneas receiving intraperitoneal vehicle injections. These findings confirmed the important role of MMP-8 induced by Dex in controlling inflammation after corneal alkali burns.

In conclusion, our data show that MMP-8 is required for the anti-inflammatory effects of Dex in limiting inflammation and preserving corneal clarity following corneal injury. This work sheds light on the biological function of MMP-8, in the protective effects of Dex in corneal wound healing in the severe inflammation induced by alkali burn and dry eye. Safer and more efficient anti-inflammatory therapies may not aim to decrease all MMPs, since we showed that MMP-8 can have protective functions during Dex treatment.

Acknowledgments

Abbreviations

AB	alkali burn
DS	desiccating stress
CM	combined model (AB + DS)
D	days
UT	untreated
MMP	matrix metalloproteinase
MPO	myeloperoxidase
IL	interleukin
B6	C57BL/6
QID	*quater in die* (in Latin, 4 times a day)
QD	*quaque die* (in Latin, every day)
IP	intraperitoneal
KO	knock out
Dex	dexamethasone

BSS	balanced salt solution
CXCL1	C-X-C motif ligand 1
WT	wild type

Literature Cited

Al-Moujahed A, Chodosh J. Outcomes of an algorithmic approach to treating mild ocular alkali burns. JAMA Ophthalmol. 2015; 133(10):1214–1216. [PubMed: 26226389]

Albietz J, Douglas I, Napper G. Ocular therapeutics. Clin Exp Optom. 2007; 90:141–142. [PubMed: 17311577]

Astrom P, Pirila E, Lithovius R, Heikkola H, Korpi JT, Hernandez M, Sorsa T, Salo T. Matrix metalloproteinase-8 regulates transforming growth factor-beta1 levels in mouse tongue wounds and fibroblasts in vitro. Exp Cell Res. 2014; 328:217–227. [PubMed: 25036555]

Balbin M, Fueyo A, Knauper V, Pendas AM, Lopez JM, Jimenez MG, Murphy G, Lopez-Otin C. Collagenase 2 (MMP-8) expression in murine tissue-remodeling processes. Analysis of its potential role in postpartum involution of the uterus. J Biol Chem. 1998; 273:23959–23968. [PubMed: 9727011]

Bian F, Pelegrino FS, Pflugfelder SC, Volpe EA, Li DQ, de Paiva CS. Desiccating stress-induced MMP production and activity worsens wound healing in alkali-burned corneas. Invest Ophthalmol Vis Sci. 2015; 56:4908–4918. [PubMed: 26225631]

Bian F, Pelegrino FS, Tukler Henriksson J, Pflugfelder SC, Volpe EA, Li DQ, de Paiva CS. Differential effects of dexamethasone and doxycycline on inflammation and MMP production in alkali-burned corneas associated with dry eye. Ocul Surf. Jan 6.2016 2016. pii: S1542-0124(16)00002-1.

Biondo C, Mancuso G, Midiri A, Signorino G, Domina M, Lanza Cariccio V, Mohammadi N, Venza M, Venza I, Teti G, Beninati C. The interleukin-1beta/CXCL1/2/neutrophil Q8axis mediates host protection against group B streptococcal infection. Infect Immun. 2014a; 82:4508–4517. [PubMed: 25114117]

Biondo C, Mancuso G, Midiri A, Signorino G, Domina M, Lanza Cariccio V, Venza M, Venza I, Teti G, Beninati C. Essential role of interleukin-1 signaling in host defenses against group B streptococcus. mBio. 2014b; 5:e01428–e01414. [PubMed: 25205091]

Brejchova K, Liskova P, Cejkova J, Jirsova K. Role of matrix metalloproteinases in recurrent corneal melting. Exp Eye Res. 2010; 90:583–590. [PubMed: 20153319]

Chan MF, Li J, Bertrand A, Casbon AJ, Lin JH, Maltseva I, Werb Z. Protective effects of matrix metalloproteinase-12 following corneal injury. J Cell Science. 2013; 126:3948–3960. [PubMed: 23813962]

Chen L, Nakai M, Belton RJ Jr. Nowak RA. Expression of extracellular matrix metalloproteinase inducer and matrix metalloproteinases during mouse embryonic development. Reproduction. 2007; 133:405–414. [PubMed: 17307908]

Chung JH, Kang YG, Kim HJ. Effect of 0.1% dexamethasone on epithelial healing in experimental corneal alkali wounds: Morphological changes during the repair process. Graefes Arch Clin Exp Ophthalmol. 1998; 236:537–545. [PubMed: 9672801]

Corrales RM, Stern ME, de Paiva CS, Welch J, Li DQ, Pflugfelder SC. Desiccating stress stimulates expression of matrix metalloproteinases by the corneal epithelium. Invest Ophthalmol Vis Sci. 2006; 47:3293–3302. [PubMed: 16877394]

De Paiva CS, Chotikavanich S, Pangelinan SB, Pitcher JD III, Fang B, Zheng X, Ma P, Farley WJ, Siemasko KF, Niederkorn JY, et al. IL-17 disrupts corneal barrier following desiccating stress. Mucosal Immunol. 2009; 2:243–253. [PubMed: 19242409]

de Paiva CS, Corrales RM, Villarreal AL, Farley W, Li DQ, Stern ME, Pflugfelder SC. Apical corneal barrier disruption in experimental murine dry eye is abrogated by methylprednisolone and doxycycline. Invest Ophthalmol Vis Sci. 2006; 47:2847–2856. [PubMed: 16799024]

Djalilian AR, Nagineni CN, Mahesh SP, Smith JA, Nussenblatt RB, Hooks JJ. Inhibition of inflammatory cytokine production in human corneal cells by dexamethasone, but not cyclosporin. Cornea. 2006; 25:709–714. [PubMed: 17077666]

Fini ME, Girard MT, Matsubara M. Collagenolytic/gelatinolytic enzymes in corneal wound healing. Acta Ophthalmol Suppl. 1992:26–33. [PubMed: 1322008]

Gill SE, Parks WC. Metalloproteinases and their inhibitors: Regulators of wound healing. Int J Biochem Cell Biol. 2008; 40:1334–1347. [PubMed: 18083622]

Goldring MB, Otero M, Plumb DA, Dragomir C, Favero M, El Hachem K, Hashimoto K, Roach HI, Olivotto E, Borzi RM, et al. Roles of inflammatory and anabolic cytokines in cartilage metabolism: Signals and multiple effectors converge upon MMP-13 regulation in osteoarthritis. Eur Cell Mater. 2011; 21:202–220. [PubMed: 21351054]

Gooyit M, Peng Z, Wolter WR, Pi H, Ding D, Hesek D, Lee M, Boggess B, Champion MM, Suckow MA, et al. A chemical biological strategy to facilitate diabetic wound healing. ACS Chem Biol. 2014; 9:105–110. [PubMed: 24053680]

Gutierrez-Fernandez A, Inada M, Balbin M, Fueyo A, Pitiot AS, Astudillo A, Hirose K, Hirata M, Shapiro SD, Noel A, et al. Increased inflammation delays wound healing in mice deficient in collagenase-2 (MMP-8). FASEB J. 2007; 21:2580–2591. [PubMed: 17392479]

Hamill CE, Bozorg S, Peggy Chang HY, Lee H, Sayegh RR, Shukla AN, Chodosh J. Corneal alkali burns: A review of the literature and proposed protocol for evaluation and treatment. Int Ophthalmol Clin. 2013; 53:185–194. [PubMed: 24088945]

Henle P, Zimmermann G, Weiss S. Matrix metalloproteinases and failed fracture healing. Bone. 2005; 37:791–798. [PubMed: 16199217]

Herman MP, Sukhova GK, Libby P, Gerdes N, Tang N, Horton DB, Kilbride M, Breitbart RE, Chun M, Schonbeck U. Expression of neutrophil collagenase (matrix metalloproteinase-8) in human atheroma: A novel collagenolytic pathway suggested by transcriptional profiling. Circulation. 2001; 104:1899–1904. [PubMed: 11602491]

Herretes S, Suwan-Apichon O, Pirouzmanesh A, Reyes JM, Broman AT, Cano M, Gehlbach PL, Gurewitsch ED, Duh EJ, Behrens A. Use of topical human amniotic fluid in the treatment of acute ocular alkali injuries in mice. Am J Ophthalmol. 2006; 142:271–278. [PubMed: 16876508]

Hoffart L, Matonti F, Conrath J, Daniel L, Ridings B, Masson GS, Chavane F. Inhibition of corneal neovascularization after alkali burn: Comparison of different doses of bevacizumab in monotherapy or associated with dexamethasone. Clin Experiment Ophthalmol. 2010; 38:346–352. [PubMed: 21077280]

Ji KA, Eu MY, Kang SH, Gwag BJ, Jou I, Joe EH. Differential neutrophil infiltration contributes to regional differences in brain inflammation in the substantia nigra pars compacta and cortex. Glia. 2008; 56:1039–1047. [PubMed: 18381656]

Kolaczkowska E, Kubes P. Neutrophil recruitment and function in health and inflammation. Nat Rev Immunol. 2013; 13:159–175. [PubMed: 23435331]

Lin M, Jackson P, Tester AM, Diaconu E, Overall CM, Blalock JE, Pearlman E. Matrix metalloproteinase-8 facilitates neutrophil migration through the corneal stromal matrix by collagen degradation and production of the chemotactic peptide Pro-Gly-Pro. Am J Pathol. 2008; 173:144–153. [PubMed: 18556780]

Luo L, Li DQ, Doshi A, Farley W, Corrales RM, Pflugfelder SC. Experimental dry eye stimulates production of inflammatory cytokines and MMP-9 and activates MAPK signaling pathways on the ocular surface. Invest Ophthalmol Vis Sci. 2004; 45:4293–4301. [PubMed: 15557435]

Lyu J, Joo CK. Expression of Wnt and MMP in epithelial cells during corneal wound healing. Cornea. 2006; 25:S24–S28. [PubMed: 17001188]

Mitchell BM, Wu TG, Chong EM, Pate JC, Wilhelmus KR. Expression of matrix metalloproteinases 2 and 9 in experimental corneal injury and fungal keratitis. Cornea. 2007; 26:589–593. [PubMed: 17525657]

Nuti E, Panelli L, Casalini F, Avramova SI, Orlandini E, Santamaria S, Nencetti S, Tuccinardi T, Martinelli A, Cercignani G, et al. Design, synthesis, biological evaluation, and NMR studies of a new series of arylsulfones as selective and potent matrix metalloproteinase-12 inhibitors. J Med Chem. 2009; 52:6347–6361. [PubMed: 19775099]

Pflugfelder SC, Farley W, Luo L, Chen LZ, de Paiva CS, Olmos LC, Li DQ, Fini ME. Matrix metalloproteinase-9 knockout confers resistance to corneal epithelial barrier disruption in experimental dry eye. Am J Pathol. 2005; 166:61–71. [PubMed: 15632000]

Previti ML, Zhang W, Van Nostrand WE. Dexamethasone diminishes the pro-inflammatory and cytotoxic effects of amyloid beta-protein in cerebrovascular smooth muscle cells. J Neuroinflammation. 2006; 3:18. [PubMed: 16887032]

Prikk K, Maisi P, Pirila E, Sepper R, Salo T, Wahlgren J, Sorsa T. In vivo collagenase-2 (MMP-8) expression by human bronchial epithelial cells and monocytes/macrophages in bronchiectasis. J Pathol. 2001; 194:232–238. [PubMed: 11400153]

Saadat F, Khorramizadeh MR, Mirshafiey A. Apoptotic efficacy and inhibitory effect of dexamethasone on matrix metalloproteinase. Med Sci Monit. 2005; 11:BR253–BR257. [PubMed: 15990687]

Sakimoto T, Sawa M. Metalloproteinases in corneal diseases: Degradation and processing. Cornea. 2012; 31:S50–S56. [PubMed: 23038036]

Saraiya NV, Goldstein DA. Dexamethasone for ocular inflammation. Expert Opin Pharmacother. 2011; 12:1127–1131. [PubMed: 21457057]

Schrage, N.; Burgher, F.; Blomet, J.; Bodson, L.; Gerard, M.; Hall, A.; Josset, P.; Mathieu, L.; Merle, H. Chemical Q9ocular burns. Springer; 2011. p. 9-15.

Sivak JM, Fini ME. MMPs in the eye: Emerging roles for matrix metalloproteinases in ocular physiology. Prog Retin Eye Res. 2002; 21:1–14. [PubMed: 11906808]

Sosne G, Christopherson PL, Barrett RP, Fridman R. Thymosin-beta4 modulates corneal matrix metalloproteinase levels and polymorphonuclear cell infiltration after alkali injury. Invest Ophthalmol Vis Sci. 2005; 46:2388–2395. [PubMed: 15980226]

Takahashi H, Igarashi T, Fujimoto C, Ozaki N, Ishizaki M. Immunohistochemical observation of amniotic membrane patching on a corneal alkali burn in vivo. Jpn J Ophthalmol. 2007; 51:3–9. [PubMed: 17295133]

Tewari-Singh N, Jain AK, Inturi S, Ammar DA, Agarwal C, Tyagi P, Kompella UB, Enzenauer RW, Petrash JM, Agarwal R. Silibinin, dexamethasone, and doxycycline as potential therapeutic agents for treating vesicant-inflicted ocular injuries. Toxicol Appl Pharmacol. 2012; 264:23–31. [PubMed: 22841772]

Tsubota M, Sasano Y, Takahashi I, Kagayama M, Shimauchi H. Expression of MMP-8 and MMP-13 mRNAs in rat periodontium during tooth eruption. J Dent Res. 2002; 81:673–678. [PubMed: 12351664]

Weaver A, Goncalves da Silva A, Nuttall RK, Edwards DR, Shapiro SD, Rivest S, Yong VW. An elevated matrix metalloproteinase (MMP) in an animal model of multiple sclerosis is protective by affecting Th1/Th2 polarization. FASEB J. 2005; 19:1668–1670. [PubMed: 16081501]

Ye HQ, Maeda M, Yu FS, Azar DT. Differential expression of MT1-MMP (MMP-14) and collagenase III (MMP-13) genes in normal and wounded rat corneas. Invest Ophthalmol Vis Sci. 2000; 41:2894–2899. [PubMed: 10967042]

Yi K, Chung TY, Hyon JY, Koh JW, Wee WR, Shin YJ. Combined treatment with antioxidants and immunosuppressants on cytokine release by human peripheral blood mononuclear cells— Chemically injured keratocyte reaction. Mol Vis. 2011; 17:2665–2671. [PubMed: 22065919]

Yoeruek E, Ziemssen F, Henke-Fahle S, Tatar O, Tura A, Grisanti S, Bartz-Schmidt KU, Szurman P, Tubingen Bevacizumab Study G. Safety, penetration and efficacy of topically applied bevacizumab: Evaluation of eyedrops in corneal neovascularization after chemical burn. Acta Ophthalmol. 2008; 86:322–328. [PubMed: 17995975]

Zentay Z, Sharaf M, Qadir M, Drafta D, Davidson D. Mechanism for dexamethasone inhibition of neutrophil migration upon exposure to lipopolysaccharide in vitro: Role of neutrophil interleukin-8 release. Pediatr Res. 1999; 46:406–410. [PubMed: 10509360]

Zheng L, Lam WK, Tipoe GL, Shum IH, Yan C, Leung R, Sun J, Ooi GC, Tsang KW. Overexpression of matrix metalloproteinase-8 and -9 in bronchiectatic airways in vivo. Eur Respir J. 2002; 20:170–176. [PubMed: 12166566]
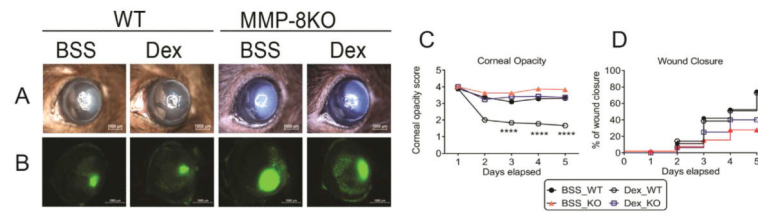
Fig. 1.
Dex treatment in MMP-8KO mice does not improve corneal clarity in a combined model of dry eye and alkali burn. A and B: Representative color digital images (A) used to score corneal opacity and representative fluorescein stained corneas (B) used to create wound closure rate and at 5D post-injury. Scale bar = 1000 μm. C and D: Corneal opacity (C) and wound closure rate (D) in corneas subjected to ocular burn with concomitant desiccating stress and topically treated with either Dex or BSS in wild-type (WT) or MMP-8KO (KO) mice. ****P< 0.0001 Dex WT versus Dex KO. Dex, Dexamethasone Sodium Phosphate; BSS, Balanced Salt Solution;
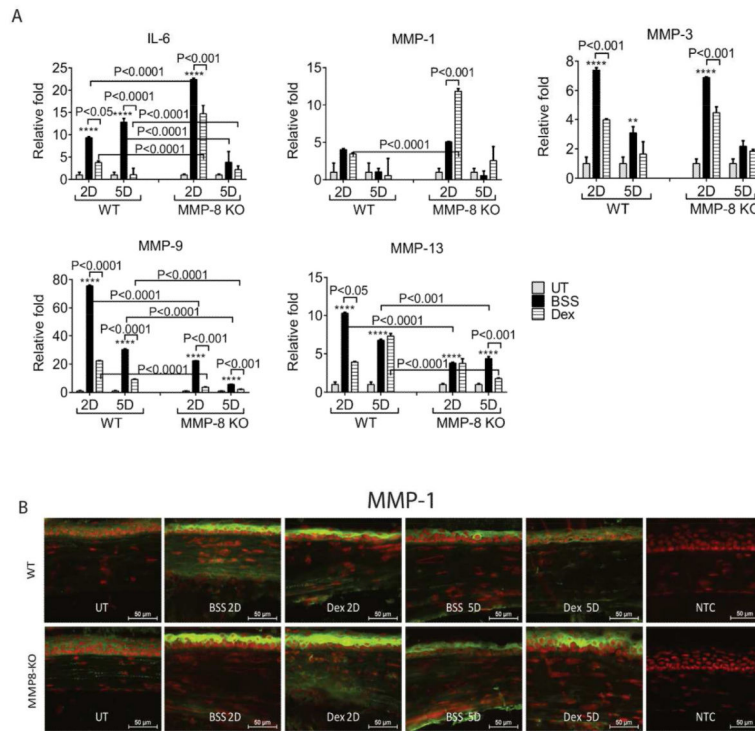
Fig. 2.
MMP-8 deficient mice failed to control inflammation with Dex treatment. A: Mean ± SEM of results of gene expression analysis of inflammatory cytokines (IL-6) and matrix metalloproteinases (MMPs) -1,-3,-9,-13 mRNA transcripts in whole cornea of animals subjected to ocular burn with desiccating stress for 2 or 5 days and topically treated with either Dex or BSS in MMP-8KO or WT mice. *P< 0.05; **P < 0.01, ***P < 0.001; ****P < 0.0001 BSS versus UT in WT, BSS versus UT in MMP-8KO. B: Representative merged pictures of MMP-1 (green) immunofluorescent staining of central cornea cryosections from animals subjected to a combined model of alkali burn and dry eye topically treated with either Dex or BSS in wild-type (WT) or MMP-8KO mice. Counterstaining was PI = red. Dex, Dexamethasone Sodium Phosphate; BSS, Balanced Salt Solution; UT= untreated control; NTC= negative control
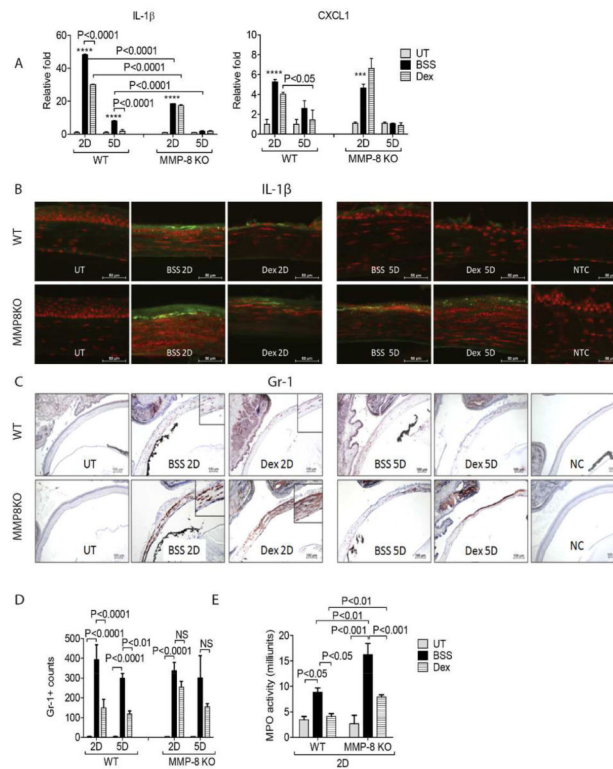
Fig. 3.
MMP-8 decreases neutrophil infiltration. A: Mean ± SEM of results of gene expression analysis of chemokines (IL-1β) and CXCL1 mRNA transcripts in whole cornea of animals subjected to ocular burn with desiccating stress for 2 or 5 days and topically treated with either Dex or BSS in MMP-8KO or WT mice. ***$P < 0.001$; ****$P < 0.0001$ BSS versus UT in WT, BSS versus UT in MMP-8KO. B: Representative merged pictures of IL-1β (green) immunofluorescent staining of central cornea cryosections from animals subjected to a combined model of alkali burn and dry eye topically treated with either Dex or BSS in wild-type (WT) or MMP-8KO mice. Counterstaining was PI = red. C: Representative pictures of Gr-1^{+} cells (red) of central cornea cryosections from animals subjected to a combined model of alkali burn and dry eye topically treated with either Dex or BSS in wild-type (WT) or MMP-8KO mice (10×). Insets are high magnification of the area below. D: Bar graphs (mean ± SEM) of Gr-1^{+} cell counts in whole cornea/groups. E: Myeloperoxidase (MPO) activity in whole corneas lysates from corneas subjected to ocular burn with concomitant desiccating stress and topically treated with either Dex or BSS in wild-type (WT) or MMP-8KO mice (mean ± SEM). Dex, Dexamethasone Sodium Phosphate; BSS, Balanced Salt Solution; UT= untreated control; NC=negative control
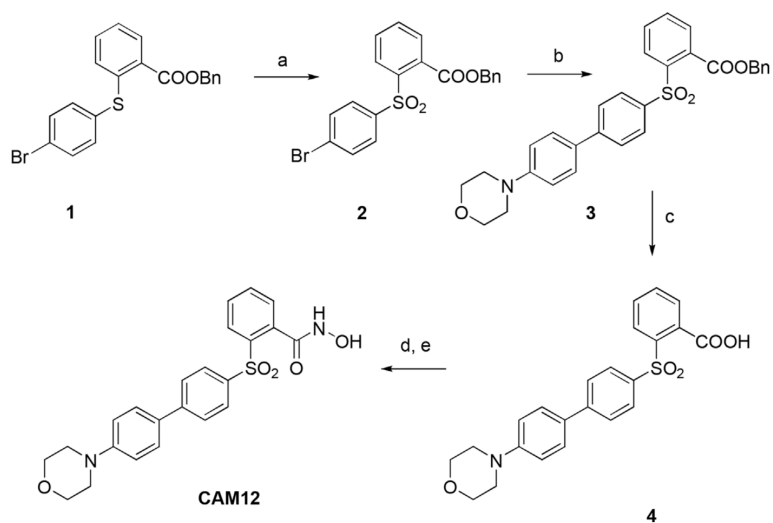
Fig. 4.
Synthetic scheme for the preparation of CAM12. Reagents and conditions: (a) Oxone, MeOH, THF, H_2O, rt; (b) 4-morpholinophenylboronic acid, $Pd(OAc)_2$, PPh_3, aqueous 2M Na_2CO_3, 1:1 EtOH/toluene, 100°C; (c) KOH, H_2O, THF, 100°C; (d) TBDMSiONH$_2$, EDC, CH_2Cl_2, rt; (e) TFA, CH_2Cl_2, 0°C.
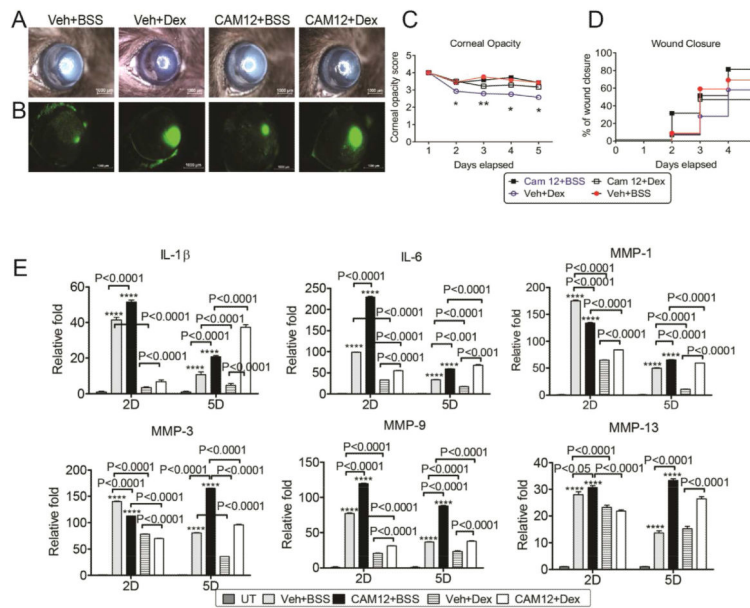
Fig. 5.
Inhibiting MMP-8 in Dex-treated corneas worsens corneal scarring in a combined model of dry eye and alkali burn. Systemic inhibition of MMP-8 increases inflammation and MMPs and decreases Dexamethasone efficacy. A and B: Corneal opacity (A) and wound closure rate (B) in corneas subjected to ocular burn with concomitant desiccating stress and topically treated with either Dex or BSS and systemic administration of vehicle or specific MMP-8 inhibitor, CAM12. *$P < 0.05$; **$P < 0.01$ Veh + Dex versus Veh + BSS. C and D: Representative color digital images used to score corneal opacity (C) and representative fluorescein stained corneas used to create wound closure rate (D) at 5D post-injury. E. Mean ± SEM of results of gene expression analysis of inflammatory cytokines (IL-6 and IL-β) and matrix metalloproteinases (MMPs) -1,-3,-9,-13 mRNA transcripts in whole cornea of animals subjected to ocular burn with desiccating stress for 2 or 5 days and topically treated with either Dex or BSS and systemic administration of BSS or specific MMP-8 inhibitor, CAM12. *$P < 0.05$; **$P < 0.01$, ***$P < 0.001$; ****$P < 0.0001$: Veh + BSS or CAM12 + BSS versus UT. Dex, Dexamethasone Sodium Phosphate; Veh, Vehicle; BSS, Balanced Salt Solution; CAM12, CAM12 MMP8 inhibitor.

TABLE 1

Oligonucleotide primers used for real-time PCR

Gene name	Symbol	Assay ID[*]
Interleukin 1 beta	IL1-β	Mm00434228
Interleukin 6	IL-6	Mm99999064
Chemokine (C-X-C motif) ligand 1	CXCL1	Mm04207460
Matrix metalloproteinase 1	MMP-1	Mm00473493
Matrix metalloproteinase 3	MMP-3	Mm00440295
Matrix metalloproteinase 8	MMP-8	Mm00439509
Matrix metalloproteinase 9	MMP-9	Mm00442991
Matrix metalloproteinase 13	MMP-13	Mm00439491
Beta-2-microglobulin	B2M	Mm00437762

[*] Identification number from Life Technologies (www.lifetechnologies.com).

TABLE 2

Dex treatment in cornea of B6 mice showed increased MMP-8 mRNA transcripts in a combined model of dry eye and alkali burn.

Time points\treatment	UT	BSS	Dex	*P*-value UT versus BSS	*P*-value BSS versus Dex
2D	1±0.31	124.52±0.51	2033.69±0.50	<0.0001	<0.0001
5D	1±0.72	110.19±0.48	319.55±0.55	<0.0001	<0.0001

Mean±SEM of relative fold of MMP-8 gene expression in whole cornea of animals subjected to ocular burn with desiccating stress for 2 or 5 days and topically treated with either Dex or BSS in WT mice.
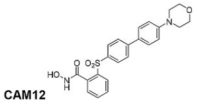
TABLE 3

In vitro^a inhibitory activity (IC$_{50}$ nM values) of hydroxamate **CAM12**

Compound/MMP	MMP-1	MMP-2	MMP-3	MMP-8	MMP-9	MMP-14
CAM12	167000	24	12000	**57**	2300	1140

^{a}The IC$_{50}$ values are the average of three determinations with SD <10%.